Published in final edited form as:
Mol Cell. 2010 December 22; 40(6): 893–904. doi:10.1016/j.molcel.2010.12.013.

Sirt3-Mediated Deacetylation of Evolutionarily Conserved Lysine 122 Regulates MnSOD Activity in Response to Stress

Randa Tao[1,2], **Mitchell C. Coleman**[1,3], **Daniel Pennington**[3], **Ozkan Ozden**[4], **Seong-Hoon Park**[4], **Haiyan Jiang**[4], **Hyun-Seok Kim**[2], **Charles Robb Flynn**[6], **Salisha Hill**[6], **W. Hayes McDonald**[6], **Alicia K. Olivier**[7], **Douglas R. Spitz**[3], and **David Gius**[4,8]

[2]Molecular Radiation Oncology, Radiation Oncology Branch, Center for Cancer Research, NCI, NIH, Bethesda, MD 20892, USA

[3]Free Radical and Radiation Biology Program, Department of Radiation Oncology, Holden Comprehensive Cancer Center, The University of Iowa, Iowa City, IA 52242, USA

[4]Departments of Radiation Oncology and Pediatrics, Vanderbilt University Medical Center, Nashville, TN 37232, USA

[5]Department of Surgery, Vanderbilt University School of Medicine, Nashville, TN 37232, USA

[6]Mass Spectrometry Research Center, Vanderbilt University School of Medicine, Nashville, TN 37232, USA

[7]Department of Pathology, Carver College of Medicine, University of Iowa, Iowa City, Iowa, USA

Abstract

Genetic deletion of the mitochondrial deacetylase sirtuin-3 (*Sirt3)* results in increased mitochondrial superoxide, a tumor permissive environment, and mammary tumor development. MnSOD contains a nutrient- and ionizing radiation (IR)-dependent reversible acetyl-lysine that is hyperacetylated in Sirt3$^{-/-}$ livers at 3 months of age. Livers of Sirt3$^{-/-}$ mice exhibit decreased MnSOD activity, but not immunoreactive protein, relative to wild-type livers. Re-introduction of wild-type, but not deacetylation null *Sirt3*, into Sirt3$^{-/-}$ MEFs deacetylated lysine and restored MnSOD activity. Site-directed mutagenesis of MnSOD lysine 122 to an arginine, mimicking deacetylation (lenti-MnSOD$^{K122\text{-}R}$), increased MnSOD activity when expressed in MnSOD$^{-/-}$ MEFs, suggesting acetylation directly regulates function. Furthermore, infection of Sirt3$^{-/-}$ MEFs with lenti-MnSOD$^{K122\text{-}R}$ inhibited *in vitro* immortalization by an oncogene (*Ras*), inhibited IR-induced genomic instability, and decreased mitochondrial superoxide. Finally, IR was unable to induce MnSOD deacetylation or activity in Sirt3$^{-/-}$ livers and these irradiated livers displayed significant IR-induced cell damage and micro-vacuolization in their hepatocytes.

Keywords

MnSOD; *Sirt3*; Mitochondria; Acetylation; Carcinogenesis

[8]Corresponding author: Department of Radiation Oncology D4105 MCN Nashville, TN 37232 David.Gius@vanderbilt.edu .
[1]The first two authors contributed equally to this manuscript.

INTRODUCTION

The incidence of human malignancies increases exponentially as a function of age, suggesting a mechanistic connection between aging and carcinogenesis (Finkel et al., 2009). Mammalian cells contain tumor suppressor (TS) genes, such as p53, and loss of TS function results in a damage permissive phenotype (Sherr and McCormick, 2002) that is an early event in carcinogenesis. *Sirt3* is one of three sirtuins localized to mitochondria (Onyango et al., 2002; Schwer et al., 2002) and is the primary mitochondrial protein deacetylase (Lombard et al., 2007). Since cancer is a disease of aging, and sirtuin genes appear to defend against cellular damage during aging, it has been proposed that *Sirt3* plays an anti-carcinogenic role and functions as a TS protein (Kim et al., 2010).

Mitochondria are thought to be central to aging and the correct function of mitochondria impedes the processes of aging and carcinogenesis by tightly regulating the reactive oxygen species generated as a byproduct of normal respiration activities (Singh, 2006). Mitochondrial abnormalities associated with altered oxidative metabolism are observed in tumor cells *in vitro* and *in vivo* and appear to contribute to a chronic condition of oxidative stress (Aykin-Burns et al., 2009). One intriguing finding from our previous work demonstrated that cells lacking *Sirt3* exhibited altered metabolism, including a significant increase in mitochondrial superoxide levels when exposed to IR. In this regard, manganese superoxide dismutase (MnSOD) is the primary mitochondrial scavenging enzyme that converts superoxide to hydrogen peroxide, which is subsequently converted to water by catalase (Spitz and Oberley, 1989). Since MnSOD enzymatically scavenges superoxide, which is increased in irradiated cells lacking *Sirt3* (Spitz and Oberley, 1989), it seemed logical to suggest that cells lacking *Sirt3* might have altered regulation of MnSOD.

Sirt3 knockout mice develop invasive ductal mammary tumors and $Sirt3^{-/-}$ mouse embryonic fibroblasts (MEFs) are easily immortalized and transformed by infection of a single oncogene (Kim et al., 2010). SIRT3 levels are also decreased in human breast malignancies, as compared to normal breast tissues, as well as in several other human malignancies (Kim et al., 2010), suggesting that *Sirt3* is a nuclear-encoded, mitochondrial-localized TS. A biochemical examination of the *in vitro* transformed $Sirt3^{-/-}$ MEFs, as well as murine tumors, strongly suggested a potential connection between aberrant mitochondrial superoxide levels and a transformation/tumor permissive cell phenotype. Specifically, a statistically significant decrease in mitochondrial MnSOD protein levels was observed at roughly one year that corresponded with the first incidence of murine mammary tumors (Kim et al., 2010). In addition, MnSOD transcription, via a mechanism involving decreased FOXO3a acetylation, was shown to decrease at roughly the same time that the first tumors were observed in the *Sirt3* knockout mice. Finally, viral overexpression of *MnSOD* prevented *in vitro* immortalization and transformation of the $Sirt3^{-/-}$ MEFs by an oncogene as well as preventing IR-induced increases in mitochondrial super oxide levels, further suggesting a role of MnSOD in the carcinogenic permissive phenotype observed in cells lacking *Sirt3*.

However, if increased mitochondrial superoxide levels play a role in carcinogenesis, it would seem logical that the decrease in MnSOD protein/activity would occur at a time point earlier than one year when it was observed that mammary tumors begin to appear in the $Sirt3^{-/-}$ animals. Thus, while the mechanistic connection between the $Sirt3^{-/-}$ mouse *in vivo* tumor permissive phenotype and increased mitochondrial superoxide seemed strong, the definition of its role as an early event in carcinogenesis seemed incomplete. Thus, we proposed that Sirt3 might regulate mitochondrial superoxide levels, via a second mechanism, which occurs much earlier than one year and is independent of total mitochondrial MnSOD protein levels. If this is the case, then loss of *Sirt3* might also result

in decreased MnSOD enzymatic activity by a post-translational mechanism, presumably via protein / lysine acetylation, which might account for the aberrant increase in mitochondrial superoxide levels, while mitochondrial MnSOD protein levels remain unchanged.

RESULTS

The kinetics of MnSOD protein levels do not correlate with mitochondrial superoxide levels

The *Sirt3* knockout mice develop tumors beginning at roughly 13 months and these tumors, as well as the *in vitro* transformed MEFs, exhibit significant aberrant mitochondrial metabolism including elevated superoxide levels (Kim et al., 2010). In this regard, a decrease in MnSOD transcription and mitochondrial MnSOD protein is also observed between 9 and 13 months in the *Sirt3* knockout mice, as compared to the wild-type mice (Fig. 1a; Supplemental Section, Fig. S1A). Interestingly, mitochondrial superoxide levels are significantly increased in the livers of $Sirt3^{-/-}$ mice at five months of age (Fig. 1b) when the levels of mitochondrial MnSOD protein in the *Sirt3* wild-type and knockout mice are identical (Fig. 1a).

Mitochondrial superoxide levels were also increased in $Sirt3^{-/-}$ MEFs at passage three, as compared to the $Sirt3^{+/+}$ MEFs (Fig. 1c) while MnSOD levels are identical (Supplemental Section, Fig. S1B). No changes in catalase activity (Supplemental Section, Fig. S1C) or catalase protein levels were observed between these mice (Fig. S1D). Thus, these results suggested that Sirt3 may be involved in the regulation, at least in part, of mitochondrial superoxide levels via a mechanism involving a post-translational modification of MnSOD. Since Sirt3 is the primary mitochondrial lysine deacetylase (Lombard et al., 2007), it seemed reasonable to propose that Sirt3 may regulate MnSOD enzymatic dismutase activity via changes in MnSOD lysine acetylation.

MnSOD contains a reversible acetyl-lysine and MnSOD activity is decreased in $Sirt3^{-/-}$ cells

Evidence that MnSOD contains reversibly acetylated lysine residues was obtained when wild-type mice at three months of age were fasted for 36 hours and liver extracts were harvested, immunoprecipitated (IPed) with an anti-MnSOD antibody, separated into equal fractions, resolved, and then immunoblotted with either an anti-acetyl (Fig. 2a, upper panel) or anti-MnSOD antibody (lower panel). These experiments showed a decrease in acetylated MnSOD (Fig. 2a, upper panel) while IPed MnSOD (lower panel) and total mitochondrial MnSOD protein levels were similar (Supplement Section, Fig. S2A). In addition, no difference in MnSOD protein acetylation (Supplemental Section, Fig. S2B, upper panel), IPed MnSOD (lower panel), or total mitochondrial MnSOD protein (Supplemental Section, Fig. S2C, lane 1 versus 3) was observed in the livers of the $Sirt3^{-/-}$ mice at three months of age or when these mice were fasted, as compared to the fed mice.

Livers from isogenic, three-month-old, age-matched wild-type and $Sirt3^{-/-}$ mice were also harvested, IPed with an anti-MnSOD antibody, separated into two equal fractions, resolved, and immunoblotted with either an anti-acetyl (Fig. 2b, upper panel) or anti-MnSOD antibody (lower panel). These results showed that MnSOD acetylation was increased in the $Sirt3^{-/-}$ livers (Fig. 2b) while no difference in total MnSOD (lower panel) or mitochondrial MnSOD (Supplemental Section, Fig. S2C, lane 1 versus 2) was observed. Nicotinamide phosphoribosyl-transferase (NAMPT) enhances cellular NAD levels and increases Sirt1 transcriptional activity in a dose-dependent manner (Revollo et al., 2004), so it seemed reasonable to determine if NAMPT levels are increased in our fasting mice and whether this induces Sirt3. Immunoblotted with an anti-NAMPT antibody showed no change in NAMPT

in the $Sirt3^{+/+}$ or $Sirt3^{-/-}$ mice or after these mice were fasted for 36 hours (Supplemental Section, Fig. S2D).

These results support the hypothesis that MnSOD is a target for reversible lysine acetylation mediated by Sirt3. Thus, MnSOD enzymatic activity was determined in the *Sirt3* knockout livers as well as MEFs, and these results showed that MnSOD activity was significantly decreased in liver tissues from $Sirt3^{-/-}$ mice at age three months and $Sirt3^{-/-}$ MEFs at passage number three (Fig. 2c-d). Total MnSOD levels were similar in the $Sirt3^{-/-}$ livers (Supplemental Section, Fig. S2C), as compared to the $Sirt3^{+/+}$ liver controls. In addition, immunoblotting with an anti-acetyl-lysine 122 MnSOD (Epitomics, Inc, Burlingame, CA) antibody (Fig. 2e) as well as mass spectrometry (Fig. 2f, Supplemental Fig. S2E) demonstrated an increase the acetylation of MnSOD lysine 122 in the livers samples from $Sirt3^{-/-}$ mice at three months of age, as compared to age-matched wild-type mice.

Re-expression of Sirt3 deacetylates MnSOD and restores superoxide dismutase activity

To determine if Sirt3 directly deacetylates MnSOD and alters enzymatic activity, two lentiviruses were constructed that expressed either the wild-type (lenti-Sirt3-wt) or a deacetylation null mutant (lenti-Sirt3-dn) *Sirt3* gene (a gift from Dr. Toren Finkel, NIDDK) in which amino acid 248 was changed from a histidine to tyrosine (Ahn et al., 2008). These viruses were used to infect $Sirt3^{-/-}$ MEFs. Infection with lenti-Sirt3-wt, but not lenti-Sirt3-dn, decreased MnSOD acetylation (Fig. 3a, lane 3 versus 4, upper panel) while infection of these lentiviruses expressed similar levels of exogenous Sirt3 wild type and mutant protein (Fig. 3b). Lenti-Sirt3-wt, but not lenti-Sirt3-dn, also increased MnSOD activity (Fig. 3c) and decreased mitochondrial superoxide levels (Fig. 3d) while the levels of IPed MnSOD were similar in the control and infected $Sirt3^{-/-}$ MEFs (Fig. 3a, lower panel). These results support the hypothesis that Sirt3 directly deacetylates MnSOD leading to increased dismutase activity.

To more rigorously determine if MnSOD is a legitimate Sirt3 deacetylation target, an *in vitro* SIRT3 deacetylation assay was performed. IPed purified MnSOD was mixed without or with purified SIRT3 with 1 mM NAD+, separated, and immunoblotting with an either an anti-acetyl, anti-SIRT3, or anti-MnSOD antibody. These experiments showed that Sirt3 decreased MnSOD acetylation (Fig. 3e, lane 1 versus 2) and removal of NAD+ (lane 3) or the addition of nicotinamide (lane 4) prevented the deacetylation of MnSOD, suggesting that SIRT3 directly deacetylates MnSOD *in vitro*. Finally, these experiments were repeated using a specific anti-MnSOD lysine 122 antibody showing that lysine 122 is deacetylated *in vitro* by SIRT3 (Fig. 3f).

SIRT3 likely interacts with MnSOD

Since Sirt3 deacetylates MnSOD it seemed reasonable to propose that these two proteins might physically interact. As such, HCT116 cells were used that have been genetically altered to overexpress a myc-tagged wild-type *Sirt3* gene ($HCT116^{myc\text{-}SIRT3wt}$ cells). These cells were lysed and IPed with either an anti-MnSOD or anti-myc antibody. The samples were divided into three equal fractions, separated, and subsequently immunoblotted with either an anti-myc (Fig. 4a, upper panel), anti-SIRT3 (middle panel), or anti-MnSOD (lower panel) antibody. Reverse IPs were also done with anti-SIRT3 (upper panel) or anti-MnSOD (lower panel) antibodies demonstrating that endogenous SIRT3 and MnSOD appear to form a protein interaction (Fig. 4b). These results suggest a potential physical interaction between Sirt3 and MnSOD. In addition, the HCT116 cells were grown on slides that were subsequently stained with anti-MnSOD, anti-SIRT3, DAPI, and mitotracker (Fig. 4c). The immunohistochemical experiments using the anti-MnSOD and anti-SIRT3 staining were also subsequently merged (Fig. 4d) and suggest that the SIRT3 and MnSOD proteins co-

localized to each other and to the mitochondria. However, these results also show areas where these proteins do not co-localize as might be expected since most enzyme/substrate interactions are highly dynamic and may be very transient.

MnSOD contains an evolutionarily conserved lysine that directly regulates activity

MnSOD is an old, evolutionarily conserved protein present in almost all species and as such, if a specific MnSOD lysine is an acetylation target in the regulation of enzymatic activity, then it seems reasonable that this lysine would be conserved in multiple mammalian and non-mammalian species. A BLAST search demonstrated a conserved 13 amino acid motif (GELLEAIK*RDFGS) around the lysine of interest at amino acid position 122 that is present in human, murine, bovine, etc. (Fig. 5a) as well as at position 121 in *C. elegans*. Interestingly, the MnSOD protein in four primates (*Rhesus macaque*, *Callithrix jacchus*, *Common gibbon*, and *Chimpanzee*) contains an identical 13 amino acid consensus motif; however, it is located 24 amino acids upstream of the human sequence and the conserved lysine is present at position 98. The consensus motif is also shifted in multiple non-mammalian species including *Xenopus tropicalis* and zebrafish to a slightly different protein location (lysine 124 versus 122) (Fig. 5a). Thus, it seems reasonable to propose that this conserved 13 amino acid motif, which has remained roughly intact in multiple species, while in some cased being moved to slightly different locations within the MnSOD protein, suggests that this lysine may be of potentially significant biological and physiological importance. Finally, an examination of the published 3-dimensional structure of the MnSOD protein (PDB accession number 1PL4), which is a functional tetramer *in vivo*, shows that lysine 122 is on the outside of the protein complex in an ideal position to interact with other proteins, such as Sirt3 (Supplemental Section, Fig. S5A).

It has previously been shown that substitution of a lysine with a glutamine mimics an acetylated amino acid state, while substitution with an arginine mimics deacetylation (Li et al., 2007; Schwer et al., 2006). Thus, mutating lysine 122 to arginine would be predicted to mimic a deacetylated lysine, while substitution with a glutamine would be expected to mimic an acetylated lysine (Fig. 5b). As such, lenti-MnSOD^{K122} (wild-type), lenti-MnSOD$^{K122\text{-}R}$, lenti-MnSOD$^{K122\text{-}Q}$, and a control virus were used to infect MEFs that have *MnSOD* genetically deleted (MnSOD$^{-/-}$ MEFs) (a kind gift from Dr. Prahbat Goswami, University of Iowa). The MnSOD$^{-/-}$ MEFs have previously been shown to have significantly increased mitochondrial superoxide levels, as compared to wild-type MEFs (Du et al., 2009).

Infection of the MnSOD$^{-/-}$ MEFs at passage 20 with the various MnSOD lentiviruses resulted in similar levels of cellular exogenous protein (Supplemental Section, Fig. S5B). In addition, infection with the K122-R mutant (lenti-MnSOD$^{K122\text{-}R}$) resulted in increased MnSOD activity (Fig. 5c) and decreased mitochondrial superoxide levels (Fig. 5d), while the K122-Q mutant displayed the opposite results, when compared to cells infected with the wild-type *MnSOD* lentivirus (Fig. 5c-d). To make a stronger mechanistic connection between Sirt3 and MnSOD lysine 122, MnSOD$^{-/-}$ MEFs were infected with the wild-type or mutant *MnSOD* viruses and lenti-Sirt3-wt or lenti-Sirt3-dn. These experiments showed that infection of wild-type *Sirt3*, but not the deacetylation null gene, increased MnSOD activity in the MnSOD$^{-/-}$ MEFs expressing wild-type *MnSOD* (Fig. 5e, bar 1 versus 2). In contrast, infection with lenti-Sirt3-wt or lenti-Sirt3-dn did not alter the activity of MnSOD in MnSOD$^{-/-}$ MEFs co-infected with either lenti-MnSODK$^{122\text{-}R}$ or lenti-MnSODK$^{122\text{-}Q}$. Finally, infection of the MnSOD$^{-/-}$ MEFs with the wild-type and mutant MnSOD expressing lentiviruses did not alter cellular H_2O_2 levels (Supplemental Section, Fig. S5C). These results suggest that acetylation of MnSOD lysine 122 directly regulates MnSOD enzymatic dismutase activity.

It has previously been shown that exposure to ionizing radiation (IR) decreases contact inhibition, as measured by increased foci formation, in *MnSOD* knockout MEFs (Du et al., 2009). Infection of the $MnSOD^{K122\text{-}R}$ mutant lentivirus into the $MnSOD^{-/-}$ MEFs (Supplemental Section, Fig. S5B) demonstrated a significant decrease in IR-induced foci formation, while the foci number in the MEFs infected with the $MnSOD^{K122\text{-}Q}$ mutant was identical to the control virus (Fig. 5f). Consistent with the idea that MnSOD activity is regulated, at least in part, by acetylation of lysine 122, infection of the $MnSOD^{-/-}$ MEFs with lenti-$MnSOD^{K122\text{-}R}$ also decreased IR-induced mitochondrial superoxide levels (as determined by MitoSOX oxidation), (Supplemental Section, Fig. S5D, lane 5 versus lane 2). In contrast, infection with lenti-$MnSOD^{K122\text{-}Q}$ resulted in MitoSOX oxidation similar to the control cells (lane 4 versus lane 2). These experiments were repeated after co-infection of the $MnSOD^{-/-}$ MEFs with either lenti-Sirt3-wt or lenti-Sirt3-dn. Overexpression of *Sirt3* decreased the number of foci in $MnSOD^{-/-}$ MEFs co-infected with lenti-$MnSOD^{K122}$ (Fig. 5g, bar 2 versus 3) to the about same number of foci observed in MEFs infected with lenti-Sirt3-wt or lenti-Sirt3-dn and lenti-$MnSOD^{K122\text{-}R}$ (bar 3 versus 4-5). In contrast, infection of lenti-Sirt3-wt or lenti-Sirt3-dn did not change the number of foci in MEFs infected with lenti-$MnSOD^{K122\text{-}R}$ or lenti-$MnSOD^{K122\text{-}Q}$.

Antimycin A, a mitochondrial electron transport chain (Complex III) inhibitor, represents a metabolic stress that shown to increase superoxide levels (Aykin-Burns et al., 2009). Exposure of $MnSOD^{-/-}$ MEFs to Antimycin A significantly increased superoxide levels (Fig. 5h, lane 1) as has been previously shown (Kim et al., 2010). Infection of the $MnSOD^{-/-}$ MEFs with lenti-$MnSOD^{K122\text{-}R}$ (lane 4), and to a lesser extent lenti-$MnSOD^{K122}$ (lane 2), prior to exposure to Antimycin A prevented the increase in mitochondrial superoxide levels. In contrast, infection with lenti-$MnSOD^{K122\text{-}Q}$ had no effect on Antimycin A-induced mitochondrial superoxide levels (lane 3), as compared to the control viral infected cells (lane 1). These results suggest that acetylation of MnSOD regulates MnSOD activity following stress, and this in turn could significantly impact oxidative stress-induced superoxide levels and foci formation, a surrogate marker of *in vitro* transformation frequency.

$MnSOD^{K122\text{-}R}$ reverses IR-induced increases in superoxide and genomic instability in $Sirt3^{-/-}$ MEFs

The tumor permissive environment seen in $Sirt3^{-/-}$ animals correlates with the observation that $Sirt3^{-/-}$ MEFs can be immortalized by overexpression of a single oncogene (*Ras* or *Myc*). In addition, exposure of $Sirt3^{-/-}$ MEFs to IR increases mitochondrial superoxide levels and genomic instability (Kim et al., 2010). When $Sirt3^{-/-}$ MEFs were infected with lenti-$MnSOD^{K122\text{-}R}$, but not with lenti-$Sirt3^{K122\text{-}Q}$, immortalization induced by lentivirus-mediated overexpression of *Ras* or *Myc* was inhibited (Supplemental Section, Table S1). Consistent with this effect being mediated by the activity of MnSOD, infection with lenti-$MnSOD^{K122\text{-}R}$, but not lenti-$MnSOD^{K122\text{-}Q}$, prevented IR-induced increases in steady-state levels of mitochondrial superoxide as determined by MitoSOX oxidation (Fig. 6a) as well as genomic instability as indicated by IR-induced changes in ploidy (Fig. 6b). Western immunoblotting confirmed similar levels of expressed exogenous wild-type and mutant MnSOD protein in the infected $Sirt3^{-/-}$ MEFs (Supplemental Section, Fig. S6A). No change in cellular H_2O_2 levels was observed in the $Sirt3^{-/-}$ MEFs infected with these MnSOD expressing lentiviruses (Supplemental Section, Fig. S6B).

We have previously shown that $Sirt3^{-/-}$ MEFs immortalized and transformed by infection with *Ras* (referred to as $Sirt3^{-/-}$ Ras cells) exhibit increased growth in soft agar, foci formation, and mitochondrial superoxide levels (Kim et al., 2010). Consistent with the results above, infection with lenti-$MnSOD^{K122\text{-}R}$, and to a lesser extent lenti-$MnSOD^{K122}$, but not lentiMnSOD$^{K122\text{-}Q}$, resulted in decreased growth in soft agar (Fig. 6c), decreased

foci formation (Fig. 6d), and decreased mitochondrial superoxide levels (Supplemental Section, Fig. S6C) in the transformed Sirt3$^{-/-}$ Ras cells. Western immunoblotting confirmed similar levels of expressed exogenous wild-type and mutant MnSOD protein in the infected Sirt3$^{-/-}$ Ras cells (Supplemental Section, Fig. S6D).

In vivo liver MnSOD activity, MnSOD acetylation, and radiosensitivity in the Sirt3$^{-/-}$ mice

The results above suggest that acetylation of MnSOD may alter *in vivo* responses to radiation exposure. In order to test this hypothesis, Sirt3$^{+/+}$ and Sirt3$^{-/-}$ mice were exposed to 2 Gy of whole body IR on 2 consecutive days and liver mitochondria were harvested 24 hours following the second exposure to radiation. These experiments showed a significant IR-induced increase in liver MnSOD activity (Fig. 7a) as well as a decrease in lysine 122 MnSOD acetylation (Fig. 7b; Supplemental Section, Fig. S7A) in liver mitochondria of Sirt3$^{+/+}$ animals. In contrast, no change in MnSOD activity or lysine acetylation was observed in the liver mitochondria isolated from IR-exposed Sirt3$^{-/-}$ mice (Fig. 7a-b). Total mitochondrial MnSOD immunoreactive protein levels in the irradiated and control groups were identical (Supplemental Section, Fig. S7B). These results support the hypothesis that Sirt3$^{-/-}$ liver mitochondria lack the capacity to induce MnSOD activity in response to IR because of an inability to deacetylate MnSOD.

If *Sirt3* knockout mice are unable to induce MnSOD activity in response to IR then it seems reasonable to hypothesize that this loss of the ability to induce a potentially protective response could result in enhanced IR-induced liver damage. As such, livers from Sirt3$^{+/+}$ and Sirt3$^{-/-}$ mice exposed to 2 Gy of radiation on two consecutive days were harvested at 24 hours. Histological examination of the irradiated *Sirt3* knockout mice exposed to IR demonstrated marked periportal to midzonal hepatocellular swelling with dilation of the cytoplasm by clear space as well as poorly defined vacuoles (Fig. 7c). Hepatocellular swelling in the irradiated Sirt3$^{-/-}$ mice livers was significant more severe as compared to the irradiated Sirt3$^{+/+}$ or the control Sirt3$^{+/+}$ and Sirt3$^{-/-}$ mice (Fig. 7d). Liver sections processed with osmium tetroxide (stains lipid in fixed tissue) demonstrated minimal to no lipid vacuoles in the swollen hepatocytes of Sirt3$^{-/-}$ mice (Supplemental Section, Fig. S7D, top panels). In addition, liver sections from irradiated Sirt3$^{-/-}$ mice were stained with Periodic Acid-Schiff (PAS) (stains glycogen) demonstrated mild to moderate cytoplasmic glycogen with poorly defined clear spaces (Fig. S7D, bottom panels). This histology is displays some characteristics similar to, at least in part, that observed in microvesicular steatosis that is associated with mitochondrial dysfunction (Araya et al., 2006). Interestingly, the risk factors for steatosis include diabetes mellitus, protein malnutrition, and obesity (Araya et al., 2006), all of which have been associated with abnormalities of Sirtuin function (Finkel et al., 2009).

When the livers from these mice were stained with markers for apoptosis the *Sirt3* knockout mice exposed to irradiation demonstrated significantly more apoptosis then the irradiated wild-type mice as well as the control Sirt3$^{+/+}$ and Sirt3$^{-/-}$ mice as measured by TUNEL assay (Fig. 7e) or staining with antibodies to cleaved caspase-3 (Supplemental Section, Fig. S7C). This result is consistent with the increased cellular damage and the membrane bound vacuoles observed in the H & E staining (Tolman and Dalpiaz, 2007).

Control and irradiated Sirt3$^{+/+}$ and Sirt3$^{-/-}$ livers were also stained with an anti-nitrotyrosine antibody as a marker for increased protein damage caused by intracellular reactive oxygen/nitrogen species, specifically $ONOO^{-}$, a reaction product of nitric oxide and superoxide (Kim et al., 2010). *Sirt3* knockout mouse liver cells exhibited increased anti-nitrotyrosine staining (Fig. 7f, bar 1 versus 3), as compared the Sirt3$^{+/+}$ samples (quantified in Supplemental Fig. S7E, $P < 0.05$), and there was a very significant difference between the Sirt3$^{+/+}$ and Sirt3$^{-/-}$ irradiated liver samples (bar 2 versus 4, $P < 0.01$). These results

suggest an oxidative stress permissive phenotype in liver cells lacking *Sirt3* that becomes more evident upon IR-induced oxidative stress.

DISCUSSION

We have previously demonstrated that Sirt3 is an *in vitro* and *in vivo* and the knockout mice spontaneously form well differentiated, ER/PR-positive mammary tumors(Kim et al., 2010). In addition, SIRT3 protein levels are decreased in human breast cancers as well as several other human malignancies. These results identified Sirt3 as a genomically expressed, mitochondrially localized TS and cells lacking *Sirt3* may be a useful *in vivo* model to investigate the subtype of breast cancer observed in post-menopausal or older women.

One intriguing finding from our previous work was that cells lacking *Sirt3* exhibited altered mitochondrial metabolism as exhibited by increased mitochondrial superoxide levels during stress. These results suggested a connection between the increase in superoxide and the *Sirt3* knockout mouse tumor permissive phenotype. However, one outstanding question from this previous work involved the observation that MnSOD transcription, via FOXO3a acetylation, was not decreased until one year—roughly the same time that the mammary tumors were first observed in the *Sirt3* knockout mice. Thus, while the connection between the MnSOD and increased mitochondrial superoxide seemed strong, the mechanism appeared to be more complex than a decrease in FOXO3a driven MnSOD transcription (Kim et al., 2010). Thus, additional wild-type and *Sirt3* knockout mouse colonies were established and followed to more rigorously investigate the connection between superoxide levels and MnSOD as an early carcinogenic event in the *Sirt3* knockout mouse tumor permissive phenotype. These results suggested a second potential mechanism for Sirt3 regulation of MnSOD activity that is independent of *MnSOD* expression and potentially related to post-translational modification involving acetylation.

The connection between mitochondrial damage and carcinogenesis is well established; however, the mechanism appears to be complex (Singh, 2006; Wallace, 2005). In addition, it has been suggested that the mitochondria play a role in radiation induced malignancies, but the specific molecular steps are not completely understood (Du et al., 2009). One proposed mechanism involves the accumulation of mitochondrial ROS; these reactive molecules can damage numerous cellular processes, creating an environment permissive for genomic instability as well as carcinogenesis (Oberley, 2005). Since Sirt3 is the primary mitochondrial deacetylase, we hypothesized that the increase in mitochondrial superoxide levels in *Sirt3* knockout mice and MEFs exposed to stress may be due to aberrant acetylation and regulation of MnSOD enzymatic activity.

Our results identify MnSOD amino acid 122 as a reversibly acetylated lysine residue that is deacetylated by 36 hours of fasting and MnSOD acetylation is significantly increased and enzymatic activity is decreased in $Sirt3^{-/-}$ cells. In addition, MnSOD is deacetylated by Sirt3, suggesting that mitochondrial acetylation plays a role, at least in part, in regulation of MnSOD function. This idea was validated by a pair of MnSOD mutants that demonstrated increased activity when lysine 122 was changed to arginine (to mimic the deacetylated state). $MnSOD^{K122\text{-}R}$ also prevented IR-induced foci formation in $MnSOD^{-/-}$ cells and immortalization of $Sirt3^{-/-}$ MEFs by a single oncogene, as well as IR-induced genomic instability and loss of contact inhibition.

Finally, we show *in vivo* that IR induces deacetylation of MnSOD and increased enzymatic activity in irradiated wild-type mouse liver mitochondria but not in liver mitochondria of the *Sirt3* knockout mice. While it is tempting to suggest this IR-induced damage permissive phenotype is primarily due to changes in MnSOD activity, it seems likely that other Sirt3

deacetylation targets may also play a role in this histological and biochemical phenotype. This idea would fit the well established data that IR-induced damage and cytotoxicity is a multi-factorial process involving several cellular pro-reparative pathways including redox scavenging, DNA repair, and stress responding proteins. Taken together the *in vivo* and *in vitro* results suggest MnSOD enzymatic activity is regulated by acetylation during stress and that Sirt3 regulates acetylation under specific conditions associated with neoplastic transformation, including IR-induced cellular damage.

A fundamental paradigm in biology is the presence of intracellular redox sensing proteins that recognize specific cellular conditions and initiate post-translational signaling cascades (Slane et al., 2006), and these pathways activate the cellular machinery that maintains cellular homeostasis. The most common example of this is the cytoplasmic activation of kinases that phosphorylate a series of downstream targets in response to different environmental conditions, thereby minimizing any potentially permanent cellular detrimental effects (Slane et al., 2006). In this regard, lysine acetylation has recently emerged as an important and perhaps primary post-translational modification employed to regulate mitochondrial proteins (Lombard et al., 2007).

The results presented above support this hypothesis, and together with recent findings (Kim et al., 2010), suggest that mitochondrial sirtuins, including Sirt3, may function as fidelity proteins whose loss of function may result in a damage permissive phenotype that leads to neoplastic transformation. The results presented above also suggest for the first time that the superoxide scavenging enzymatic function of MnSOD is regulated by changes in specific lysine acetylation. The connection between MnSOD and carcinogenesis, as well as tumor cell resistance to anti-cancer agents, is significant, however the mechanism of action appears to be complex (Oberley, 2005; Aykin-Burns et al., 2009). The current work represents a paradigm shift in our understanding of the post-translational regulation of MnSOD enzymatic function and the mechanism of its role in responses to stress. Finally, since Sirt3 is proposed to sense nutrient deprivation and oxidative stress, it also seems logical that exposure to IR, which has previously been shown to induce both oxidative stress and mitochondrial damage (Slane et al., 2006) would activate Sirt3 as a signaling pathway to protect against persistent IR-induced metabolic stress and normal tissue damage.

Experimental Procedures

Cell lines

MEFs were isolated from E14.5 isogenic *Sirt3*$^{+/+}$ and *Sirt3*$^{+/+}$ mice and maintained in a 37 °C incubator with 5% CO_2 and 6% oxygen. MEFs and HCT-116 were cultured in McCoy's 5A media, containing 10% heat-inactivated (56°C, 30 min) FBS. Sirt3$^{+/+}$ or Sirt3$^{-/-}$ MEFs (Kim et al., 2010) infected at P3 with lentivirus expressing either *Myc*, *Ras* or *MnSOD* made by Applied Biological Materials, Inc. (Richmond, British Columbia), and pooled selected cells were used for all experiments. For lentiviral infections MEFs were infected with 5 MOI of virus.

IP and immunoblot analysis

IP with anti-MnSOD and anti-Sirt3 antibodies and the subsequent western analyses were done as previously described (Kim et al., 2010). The control for these IP experiments is normalized to rabbit IgG. In addition, the IPed MnSOD samples were divided into equal fractions, separated, and blotted with anti-acetyl or anti-MnSOD antibodies. Blots were incubated with horseradish peroxidase secondary antibody, using ECL (Amersham Biosciences, Piscataway, NJ), and visualized in a Fuji Las-3000 darkbox (FujiFilm Systems, Stamford, CT).

Statistical analysis

Data were analyzed by Student's t-test, and results were considered significant at $p<0.05$. Results are presented as mean ± S.D.

MnSOD activity

MnSOD activity was analyzed in cell homogenates prepared on ice in 50 mM potassium phosphate buffer (Spitz and Oberley, 1989). This assay is based on the competition between MnSOD and an indicator molecule for superoxide production from xanthine and xanthine oxidase, in the presence of 5 mM NaCN to inhibit CuZnSOD activity (Spitz and Oberley, 1989). See Supplemental Section, Methods.

Measurement of mitochondrial superoxide levels

Superoxide production was determined as described (Kim et al., 2010) by measuring Mito-SOX (1 μM) oxidation in cells that were cultured as described above and incubated for an additional 10 minutes before being trypsinized, resuspended, and measured by flow cytometry (see Supplemental Section). Liver samples were used to determine in vivo super oxide using frozen sections of liver were mounted and stained as described (Kim et al., 2010).

Cell foci, colony formation, and soft agar assays

For foci formation assays, cells were plated onto a 10 cm plate, grown to confluence with medium replaced every 3 days for 28 days. All results for these experiments are the mean of at least three separate experiments. For the soft agar colony formation assay, 4,000 cells were plated in 2 mL of 0.4% agar in growth medium over a 3 mL base layer of agar also in growth medium. Each culture was topped with 1-2 mL of medium every 3-5 days. After 12 days, colonies were stained with methylene blue. The colonies (>0.5-mm size) were counted after 2 weeks under a light microscope.

Chromosome Analysis

MEFs were exposed at passage four to irradiation and harvested after 72 hours. Whole-mount chromosomes were counted in a blinded fashion. Individual spreads were deemed countable if all chromosomes were clearly defined and clearly visible within a single cytoplasm as previously described (Kim et al., 2010).

Catalase enzymatic activity

Catalase activity was determined as described (Slane et al., 2006). Cell extracts containing 100 μg of protein were combined with 30 mM H_2O_2 (Fisher Scientific, Suwanee, GA) in 1 mL of 50 mM potassium phosphate buffer (pH 7.0). H_2O_2 disappearance was measured at 240 nm for 120 s and recorded over 15-s intervals. Catalase enzymatic activity was expressed in k units per μg protein per second (k units/μg); $k = 1/60 \times \ln(A0/A60)$ where A0 is the initial absorbance and A60 is the absorbance at 60 s.

Liver Histopathology Examination, TUNEL Assay, and Cleaved Caspase-3 IHC

Liver sections were fixed in 10% neutral buffered formalin. Fixed tissues were then processed, paraffin embedded and sectioned at 4 μm. Sections were stained with hematoxylin and eosin or Periodic Acid Schiff reagent (for glycogen evaluation). H&E slides were scored in a blinded fashion for severity of hepatocellular vacuolation. The vacuolar change, when present, was focused in perioportal to midzonal hepatocytes therefore scoring was based on an average of 3 periportal areas per liver section. For each periportal area, 100 hepatocytes were counted and given a vacuolar severity score of low,

medium, high. Low vacuolar change was characterized by mild poorly defined cytoplasmic vacuolation consistent with glycogen accumulation. Hepatocytes with medium or high vacuolation were moderately to markedly enlarged due to dilation of the cytoplasm by clear space and few poorly defined clear vacuoles. Osmium tetroxide staining for lipid (to identify hepatocellular lipid vacuoles) was performed on formalin fixed tissues. Formal fixed tissues (3 mm) were placed in a potassium dichromate (5%)/osmium tetroxide (2%) for 7 hours followed by a 2 hour tap water rinse. Tissue sections were then routinely processed, paraffin embedded and sectioned.

TUNEL assay was performed using the ApopTag Peroxidase ISOL Apoptosis Detection Kit (Millipore, MA) according to the manufacturer's instructions. Apoptosis was detected by IHC for cleaved caspase-3 on formalin-fixed, paraffin-embedded liver tissues. Cleaved caspase-3 antibody, which is indicative of activated caspase-3, (rabbit monoclonal 1:50; Cell Signaling Technologies, Danvers, MA) was applied for 1 hour. Following several rinses, secondary antibody (Rabbit Envision HRP System; DAKO, Carpinteria, CA) and chromogen (Rabbit Envision HRP System reagents, DAB Plus and DAB Enhancer; DAKO) kits were applied as per manufacturer's instructions. TUNEL and caspase-3 staining was quantified by counting positive cells per 200X field. A total of 10 – 200X fields were counted and means of these counts were calculated for further statistical analysis.

Supplementary Material

Refer to Web version on PubMed Central for supplementary material.

Acknowledgments

DG is supported by 1R01CA152601-01 from the NCI, BC093803 from the DOD, and SPORE P50CA98131. DRS, AKO, and MCC were supported by grants from the NIH and DOE (R01CA133114, T32CA078586, P30CA086862, and DE-SC0000830). We thank Melissa Stauffer, PhD, of Scientific Editing Solutions, for editorial assistance.

REFERENCES

Ahn BH, Kim HS, Song S, Lee IH, Liu J, Vassilopoulos A, Deng CX, Finkel T. A role for the mitochondrial deacetylase Sirt3 in regulating energy homeostasis. Proc Natl Acad Sci U S A. 2008; 105:14447–14452. [PubMed: 18794531]

Aykin-Burns N, Ahmad IM, Zhu Y, Oberley LW, Spitz DR. Increased levels of superoxide and H2O2 mediate the differential susceptibility of cancer cells versus normal cells to glucose deprivation. Biochem J. 2009; 418:29–37. [PubMed: 18937644]

Du C, Gao Z, Venkatesha VA, Kalen AL, Chaudhuri L, Spitz DR, Cullen JJ, Oberley LW, Goswami PC. Mitochondrial ROS and radiation induced transformation in mouse embryonic fibroblasts. Cancer Biol Ther. 2009; 8

Finkel T, Deng CX, Mostoslavsky R. Recent progress in the biology and physiology of sirtuins. Nature. 2009; 460:587–591. [PubMed: 19641587]

Kim HS, Patel K, Muldoon-Jacobs K, Bisht KS, Aykin-Burns N, Pennington JD, van der Meer R, Nguyen P, Savage J, Owens KM, et al. SIRT3 Is a Mitochondria-Localized Tumor Suppressor Required for Maintenance of Mitochondrial Integrity and Metabolism during Stress. Cancer cell. 2010; 17:41–52. [PubMed: 20129246]

Li X, Zhang S, Blander G, Tse JG, Krieger M, Guarente L. SIRT1 deacetylates and positively regulates the nuclear receptor LXR. Molecular cell. 2007; 28:91–106. [PubMed: 17936707]

Lombard DB, Alt FW, Cheng HL, Bunkenborg J, Streeper RS, Mostoslavsky R, Kim J, Yancopoulos G, Valenzuela D, Murphy A, et al. Mammalian Sir2 homolog SIRT3 regulates global mitochondrial lysine acetylation. Mol Cell Biol. 2007; 27:8807–8814. [PubMed: 17923681]

Oberley LW. Mechanism of the tumor suppressive effect of MnSOD overexpression. Biomed Pharmacother. 2005; 59:143–148. [PubMed: 15862707]

Onyango P, Celic I, McCaffery JM, Boeke JD, Feinberg AP. SIRT3, a human SIR2 homologue, is an NAD-dependent deacetylase localized to mitochondria. Proc Natl Acad Sci U S A. 2002; 99:13653–13658. [PubMed: 12374852]

Revollo JR, Grimm AA, Imai S. The NAD biosynthesis pathway mediated by nicotinamide phosphoribosyltransferase regulates Sir2 activity in mammalian cells. J Biol Chem. 2004; 279:50754–50763. [PubMed: 15381699]

Schwer B, Bunkenborg J, Verdin RO, Andersen JS, Verdin E. Reversible lysine acetylation controls the activity of the mitochondrial enzyme acetyl-CoA synthetase 2. Proc Natl Acad Sci U S A. 2006; 103:10224–10229. [PubMed: 16788062]

Schwer B, North BJ, Frye RA, Ott M, Verdin E. The human silent information regulator (Sir)2 homologue hSIRT3 is a mitochondrial nicotinamide adenine dinucleotide-dependent deacetylase. J Cell Biol. 2002; 158:647–657. [PubMed: 12186850]

Sherr CJ, McCormick F. The RB and p53 pathways in cancer. Cancer cell. 2002; 2:103–112. [PubMed: 12204530]

Singh KK. Mitochondria damage checkpoint, aging, and cancer. Ann N Y Acad Sci. 2006; 1067:182–190. [PubMed: 16803984]

Slane BG, Aykin-Burns N, Smith BJ, Kalen AL, Goswami PC, Domann FE, Spitz DR. Mutation of succinate dehydrogenase subunit C results in increased O2.-, oxidative stress, and genomic instability. Cancer Res. 2006; 66:7615–7620. [PubMed: 16885361]

Spitz DR, Oberley LW. An assay for superoxide dismutase activity in mammalian tissue homogenates. Analytical biochemistry. 1989; 179:8–18. [PubMed: 2547324]

Tolman KG, Dalpiaz AS. Treatment of non-alcoholic fatty liver disease. Ther Clin Risk Manag. 2007; 3:1153–1163. [PubMed: 18516264]

Wallace DC. Mitochondria and cancer: Warburg addressed. Cold Spring Harbor symposia on quantitative biology. 2005; 70:363–374.

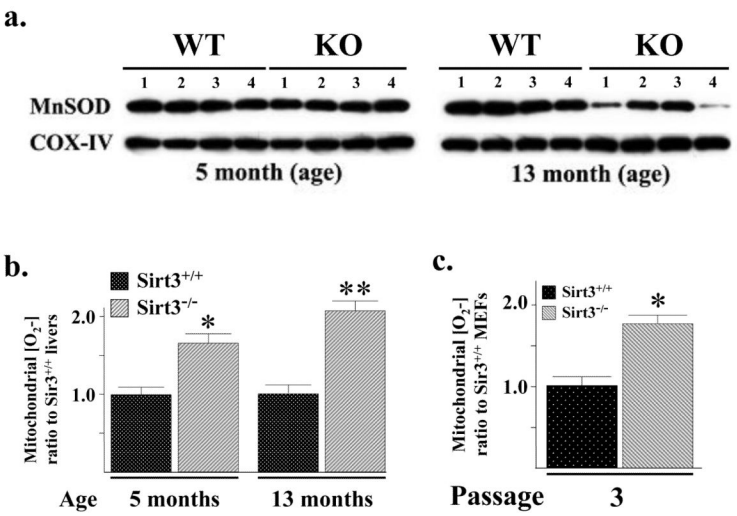

Figure 1. MnSOD protein and superoxide levels in *Sirt3* wild-type and knockout mouse livers and MEFs

(a) Livers from four Sirt3$^{+/+}$ and Sirt3$^{-/-}$ mice at 5 and 13 months of age were harvested and mitochondrial extracts were made. Lysates were separated by SDS-PAGE, transferred onto nitrocellulose, and processed for immunoblotting with an anti-MnSOD antibody (Santa Cruz Biotechnology, Inc). **(b)** Mitochondrial superoxide levels, assessed using MitoSOX oxidation, were determined in the *Sirt3* wild-type and knockout mouse livers at 5 and 13 months of age. Superoxide levels were measured as previously described (Li et al., 2001). **(c)** Mitochondrial superoxide levels were determined in the in wild-type and Sirt3$^{-/-}$ MEFs using MitoSOX oxidation at culture passage number three as previously described (Kim et al., 2010). Results in this figure are the mean of at least three separate experiments. Error bars represent one standard deviation. * indicates $P < 0.05$ and ** indicates $P < 0.01$ by t-test.

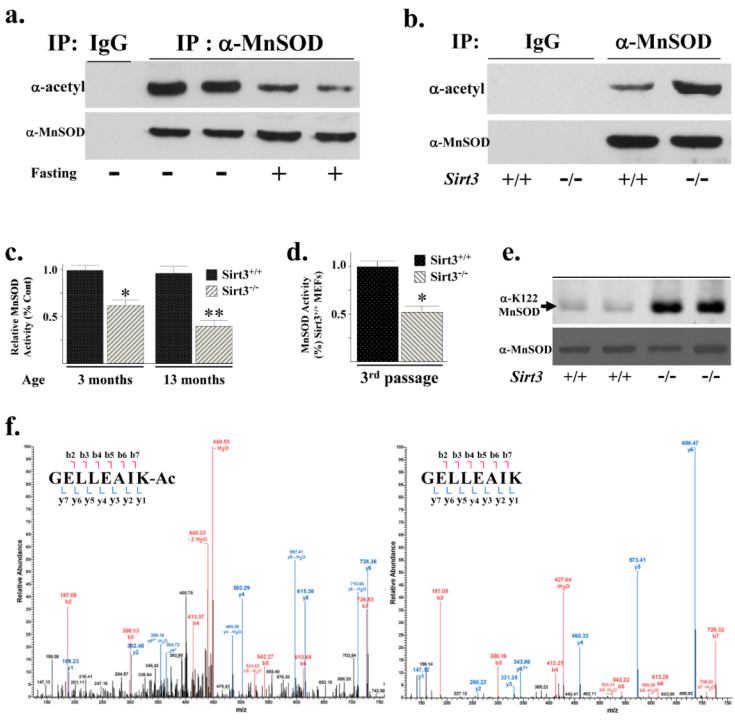

Figure 2. MnSOD contains a reversibly acetylated lysine residue and protein deacetylation and SOD activity are decreased in *Sirt3*$^{-/-}$ cells

(a) Isogenic, three-month-old age-matched Sirt3$^{+/+}$ mice were fasted for 36 hours and livers were harvested, IPed with an anti-MnSOD antibody (Santa Cruz Biotechnology, Inc), separated into two equal fractions, and subsequently immunoblotted with an anti-acetyl (Abcam) or anti-MnSOD antibody. **(b)** Livers from isogenic, three-month-old age-matched Sirt3$^{+/+}$ and Sirt3$^{-/-}$ mice were harvested, IPed with an anti-MnSOD antibody, separated into two equal fractions, and immunoblotted with either an anti-acetyl or anti-MnSOD antibody. Representative gels are shown for a-b. **(c)** MnSOD activity in *Sirt3* wild-type and knockout mouse livers at 3 and 13 months of age and **(d)** MEFs at passage number three. MnSOD activity was measured via a competitive inhibition assay as describe (Spitz and Oberley, 1989). Activity data for MnSOD is presented as units of SOD activity per milligram of protein. Results in this figure are the mean of at least three separate experiments. Error bars represent one standard deviation. * indicates $P < 0.05$ and ** indicates $P < 0.01$ by t-test. **(e)** Livers from isogenic, three-month-old age-matched Sirt3$^{+/+}$ and Sirt3$^{-/-}$ mice were harvested and immunoblotted with an anti-K122-MnSOD antibody (Epitomics, Inc - The Rabbit Monoclonal Antibody Company, recently produced for the laboratory). **(f)** Tandem mass spectrum from MnSOD demonstrates acetylated lysine 122 i*n vivo*. Liver mitochondria from wild-type and Sirt3$^{-/-}$ mice were resolved by SDS-PAGE followed by in-gel trypsin digestion, separation by nano-scale reverse-phase chromatography on reverse-phase columns and analyzed by OrbiTrap analyser via an electro-spray interface See Supplemental Section, Methods for complete description. The spectrum represents the fragmentation of the m/z's of the MnSOD peptide sequences GELLEAIK (+2 charge = 436.7580 monoisotopic mass) and GELLEAIK-ac (+2 charge= 457.7633 monoisotopic mass).

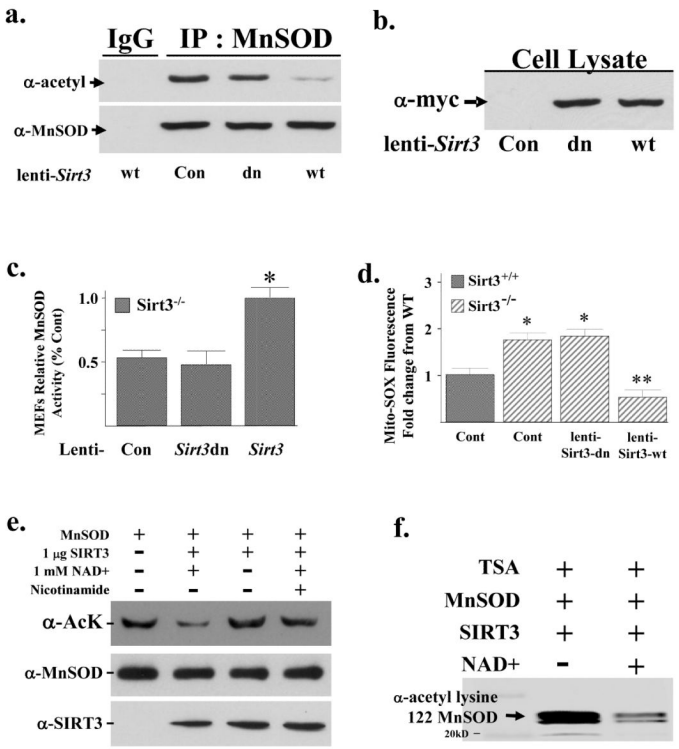

Figure 3. Re-expression of *Sirt3* in Sirt3$^{-/-}$ MEFs deacetylates MnSOD and restores SOD activity

(a) Expression of wild-type, but not a deacetylation null mutant of *Sirt3*, deacetylates MnSOD. Third passage Sirt3$^{-/-}$ MEFs were transfected with a control lentivirus, virus expressing a wild-type *Sirt3* (lenti-Sirt3-wt), or deacetylation null gene (lenti-Sirt3-dn). Forty hours after infection, Sirt3$^{-/-}$ MEFs were harvested and mitochondrial extracts were IPed with an anti-MnSOD antibody, separated into two equal fractions, and immunoblotted with either an anti-acetyl or anti-MnSOD antibody. (b) The mitochondrial samples above were also were also separated and immunoblotted with an anti-myc antibody (Santa Cruz Biotechnology, Inc). **(c)** Expression of wild-type, but not a deacetylation null mutant *Sirt3* gene increases mitochondrial MnSOD activity. Whole cell homogenates from Sirt3$^{-/-}$MEFs were infected with lenti-Sirt3-wt or lenti-Sirt3-dn and assayed for MnSOD activity in 50 mM potassium phosphate buffer. MnSOD activity was determined using an indirect competitive inhibition assay as described in the methods section (Spitz and Oberley, 1989). Results in this figure are the mean of at least three separate experiments and error bars represent one standard deviation. * indicates $P < 0.05$ by t-test. **(d)** Expression of wild-type, but not a deacetylation null mutant *Sirt3* gene, decreases mitochondrial superoxide levels. Mitochondrial superoxide levels were determined, after infection as described above, by the addition of Mito-SOX (1 μM) to the cells followed by incubation for an additional 10 minutes before being trypsinized and resuspended. Fluorescence was measured via flow cytometry. **(e)** SIRT3 directly deacetylates MnSOD *in vitro*. IPed purified MnSOD was mixed without (lane 1) or with (lanes 2-4) recombinant human SIRT3 with NAD+ (lanes 2 and 4) or nicotinamide (lane 4) and incubated. Samples were separated followed by immunoblotting with an anti-acetyl antibody. Immunoblotting for SIRT3 and MnSOD were done as internal controls. (f) IPed purified MnSOD was mixed with recombinant human SIRT3 without and with NAD+ were separated and immunoblotted with an anti-K122-MnSOD antibody (Epitomics, Inc - The Rabbit Monoclonal Antibody Company.

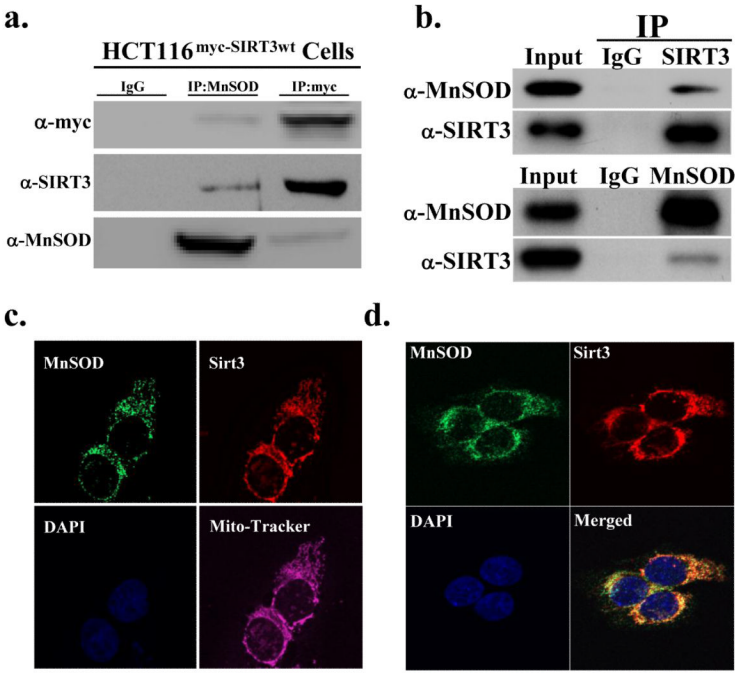

Figure 4. Sirt3 appears to interact with MnSOD in the mitochondria

(a) HCT116$^{myc\text{-}Sirt3}$ cells that are genetically altered to overexpress a myc-tagged wild-type *Sirt3* gene and **(b)** HCT116 cells were harvested and IPed with an anti-SIRT3 or an anti-MnSOD antibody and separated into equal fractions. The samples were resolved and immunoblotted with either an anti-SIRT3 or anti-MnSOD antibody. HCT116 cells were stained with an **(c)** anti-SIRT3 and anti-MnSOD antibody as well as with DAPI and mitotracker or with **(d)** an anti-SIRT3 and anti-MnSOD antibody and DAPI and the images were merged. Representative gels or micrographs for this figure are shown. Results for the panels in this figure are the mean of at least three separate experiments. Error bars represent one standard deviation. * indicates $P < 0.05$ by t-test.

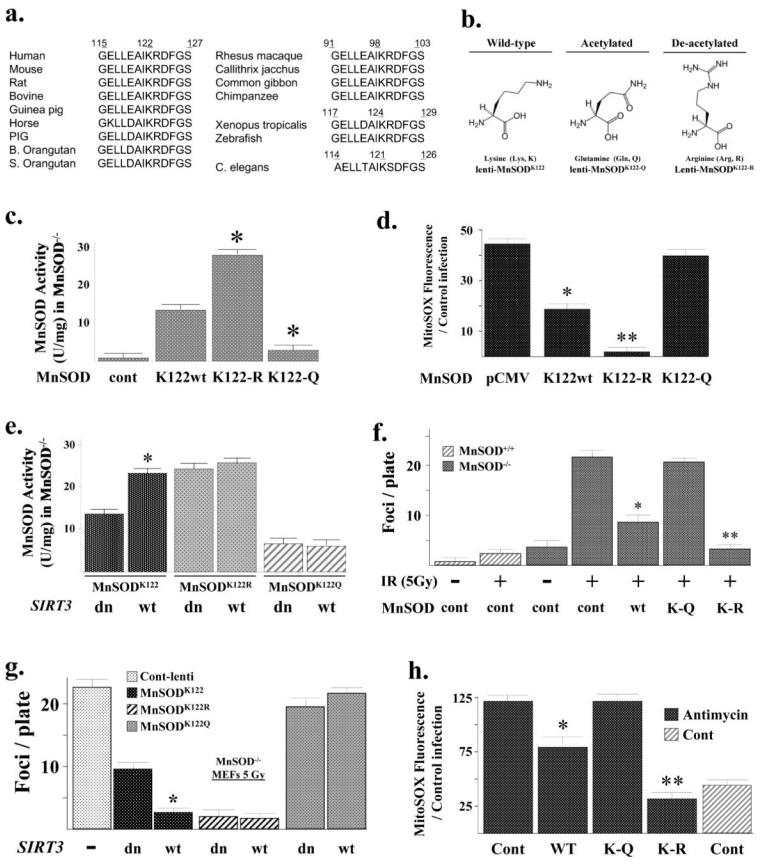

Figure 5. MnSOD contains an evolutionarily conserved lysine residue that regulates SOD activity

(a) Multiple species contain a potentially reversibly acetylated lysine residue. The MnSOD protein sequence from multiple species was BLASTed based on the reversibly acetylated lysine located at amino acid 122 in mice. A 13-amino acid motif (GELLEAIK*RDFGS) was identified that is present in multiple species. **(b)** Substitution of a lysine with a glutamine (Q) mimics an acetylated amino acid state, while substitution with an arginine (R) mimics a deacetylated amino acid state (Li et al., 2007; Schwer et al., 2006). **(c)** MnSOD lysine acetylation status directs dismutase activity. MnSOD$^{-/-}$ MEFs were infected with a control lentivirus or lenti-MnSOD^{wt}, lenti-MnSOD$^{K122\text{-}Q}$, or lenti-MnSOD$^{K122\text{-}R}$. Twenty-four hours after infection, MnSOD activity was determined as outlined above (Fig. 3 legend). **(d)** Mitochondrial superoxide levels are decreased in cells overexpressing a *MnSOD$^{K122\text{-}R}$* mutant gene. MnSOD$^{-/-}$ MEFs were infected with the various MnSOD lentiviruses and superoxide levels were determined as described above. **(e)** MnSOD$^{-/-}$ MEFs were infected with the wild-type and mutant MnSOD lentiviruses with either lenti-Sirt3-wt or lenti-Sirt3-dn and assayed for MnSOD activity. **(f)** The MnSOD$^{K122\text{-}R}$ mutant decreases IR-induced contact inhibition in the *MnSOD* knockout MEFs. MnSOD$^{-/-}$ MEFs were infected with the MnSOD lentiviruses, plated at 1×10^6/100 mm dish, exposed to 5 Gy IR, followed by long-term culture (28 days), staining with crystal violet, and measurement of foci formation. **(g)** MnSOD$^{-/-}$ MEFs were infected with the wild-type and mutant MnSOD lentiviruses with either lenti-Sirt3-wt or lenti-Sirt3-dn and measured for foci formation as above. **(h)** Mitochondrial superoxide levels in MnSOD$^{-/-}$ MEFs exposed to Antimcyin A are decreased by infection with lenti-MnSOD$^{K122\text{-}R}$, Sirt3$^{-/-}$ MEFs were treated with 5 μM of Antimycin A for 3 hours and mitochondrial superoxide levels were determined as described above. Results for all the panels in this figure are the mean of at least three separate

experiments and error bars represent one standard deviation. * indicates $P < 0.05$ and ** indicates $P < 0.01$ by t-test.

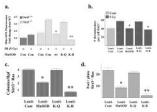

Figure 6. The MnSOD^{K122-R} mutant reverses the increase in IR-induced superoxide levels and genomic instability in the primary or *Ras* transformed Sirt3$^{-/-}$ MEFs

(a) Wild-type and Sirt3$^{-/-}$ MEFs were exposed to 5 Gy of IR and mitochondrial superoxide levels were determined by the addition of Mito-SOX (1 μM) to the cells. **(b)** The MnSOD^{K122-R} mutant prevents aneuploidy in *Sirt3* knockout MEFs exposed to IR. Sirt3$^{-/-}$ MEFs were infected with a control lentivirus or lenti-MnSOD^{wt}, lenti-MnSOD^{K122-Q}, or lenti-MnSOD^{K122-R} and exposed to 5 Gy of IR. Whole-mount chromosomes were counted in a blinded fashion. Bars show the mean chromosome number per cell from 100 separate counts. **(c-d)** The MnSOD^{K122-R} mutant reverses the transformed phenotype in Sirt3$^{-/-}$ MEFs infected with *Ras*. The transformed Sirt3$^{-/-}$ Ras cells were transfected with the *MnSOD* lentiviruses outlined above, and **(c)** growth in soft agar and **(d)** spontaneous foci formation were determined as described above. For growth in soft agar, Sirt3$^{-/-}$ Myc/Ras cells were seeded and colonies were stained with methylene blue after 12 days and counted. Results for all the panels in this figure are the mean of at least three separate experiments and error bars represent one standard deviation. * indicates $P < 0.05$ and ** indicates $P < 0.01$ by t-test.

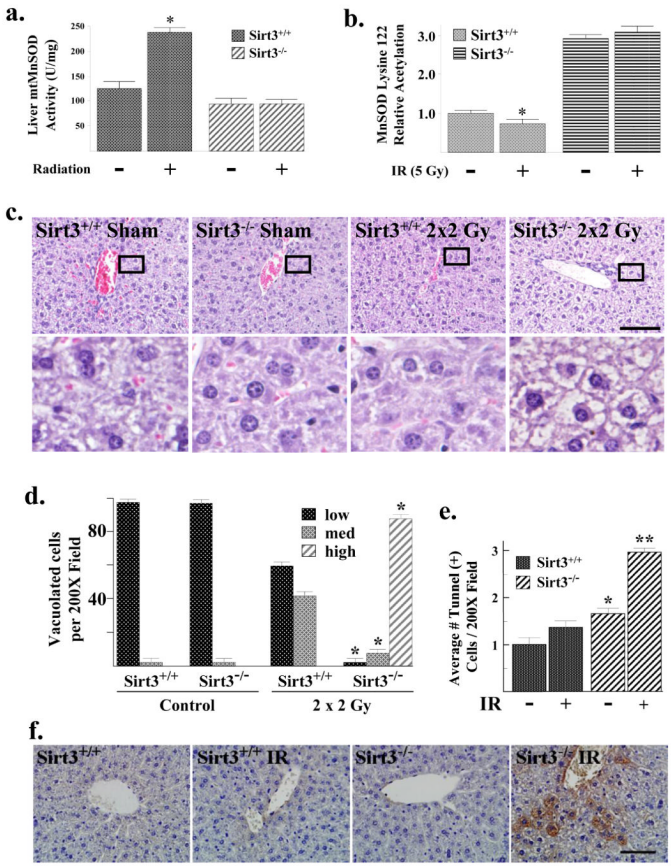

Figure 7. MnSOD dismutase activity, lysine 122 acetylation, and the cellular metabolic and damage/cytotoxic response are altered by IR

(a) Sirt3$^{+/+}$ and Sirt3$^{-/-}$ mice at 12 weeks were exposed to sham or 2 × 2 Gy exposure every 24 hours. Livers were harvested 20 hours post-exposure, and mitochondria were isolated. MnSOD activity in MEFs was measured via a competitive inhibition assay as described (Spitz and Oberley, 1989). Activity data for MnSOD is presented as units of SOD activity per milligram of protein. **(b)** Mitochondrial extracts from above were analyzed for acetylation of MnSOD lysine 122 via mass spectrometry. Results are presented as fold change from the untreated, wild-type mouse livers. **(c)** Sirt3$^{-/-}$ mouse livers exposed to IR exhibit marked cytoplasmic vacuolation of periportal to midzonal hepatocytes. The wild-type and Sirt3$^{-/-}$ livers without and with exposure to IR were H & E stained and scored for degree of hepatocellular cytoplasmic vacuolation; low, medium and high by a pathologist (AKO). Representative micrographs are shown. Scale bar = 80 μm. (d) Quantification of the H & E for liver cells. Liver cells were scored as low = no detectable cytoplasmic vacuolation, med = moderate dilation of the cytoplasm by clear space primarily affecting periportal hepatocytes, high = severe dilation of the cytoplasm by clear space and poorly defined clear vacuoles primarily affecting periportal to midzonal hepatocytes. **(e)** Apoptosis was determined in the Sirt3$^{+/+}$ and Sirt3$^{-/-}$ livers exposed to IR. Apoptotic cells were identified in liver sections by TUNEL assay. Sections were scored by a pathologist blinded to the groupings. TUNEL-positive cells were counted in 10 randomly selected 200X fields per liver section. Results in this figure are reported as the average number of positive cells per field. Data are presented as the average +/− SD. * indicates $P < 0.05$ and ** indicates $P < 0.01$. **(f)** Irradiated Sirt3$^{-/-}$ mouse liver cells exhibit increased anti-nitrotyrosine IHC staining. Liver tissue from wild-type and Sirt3$^{-/-}$ mice were stained with an anti-

nitrotyrosine antibody (StressMarq Biosciences Inc.). A representative micrograph is shown. Scale bar = 80 μm. See Figure S7E for quantification.